JJMIE

Volume 16, Number 1, January. 2022
ISSN 1995-6665
Pages 53 - 62

Jordan Journal of Mechanical and Industrial Engineering

# Dynamic Response Analysis of the Impact Force of Steel Wheel on the Elastic Half-Space

Zhipo Cao[1,2], Naixing Liang[1*], Sheng Zeng[1], Xianshui Gang[3]

[1]School of Civil Engineering, Chongqing Jiaotong University, Chongqing 400074, China
[2]Department of Automobile Engineering, Dezhou Vocational and Technical College, Dezhou 253000, China
[3]Department of Architectural Engineering, Dezhou Vocational and Technical College, Dezhou 253000, China

Received 14 July 2021 Accepted 24 December 2021

**Abstract**

In order to discover the dynamic response of the impact force of steel wheel on elastic half-space, and to quantify the peak impact force and detect the elastic modulus of elastic half-space, a finite element model of the steel wheel impacting the elastic half-space is established. According to Palmgren empirical formula, take the impact height (h), elastic modulus (E) and Poisson's ratio (σ) of elastic half-space as the main influencing factors, and take the peak acceleration of steel wheel during the impact process as the research object. The process of impacting the elastic half-space with different elastic modulus and Poisson's ratio by the same steel wheel falling at different heights is simulated by finite element method. Then, the MAP diagram and fitting formula of the relationship between peak acceleration and main influencing factors are obtained. The results show that when the steel wheel impacts the elastic half-space, there is a quadratic nonlinear relationship between the peak acceleration and impact height of steel wheel and elastic modulus of elastic half-space, and the Poisson's ratio of elastic half-space has little effect on the peak acceleration of steel wheel. The error between the theoretical values and the interpolation as well as the simulation values are around 25%, meeting the engineering requirements. So it can be used in the calculation of dynamic process of impact force that steel wheel imposes on the elastic half-space. It can be seen that the peak acceleration of steel wheel is correlated with the main influencing factors during the impact process. The impact force and the elastic modulus of elastic half-space can also be predicted according to the fitting relationship.



*Keywords:* Steel wheel; elastic half-space; impact height; elastic modulus; peak acceleration;

## 1. Introduction

Collisional impact between moving objects is a common problem in engineering, and the study of impact process has always been an often discussed and difficult issue in the field of dynamics [1]. Steel wheel is a cylindrical component commonly seen in engineering. The impact between steel wheel and plane is a typical reflection of the impact between cylinder and plane in reality. Normally, in reality the plane is multi-layer structures, which can be considered as an equivalence to the elastic half-space structure [2]. Acceleration signal is an important parameter for it is easy to measure in the dynamic response, and can fully reflect the dynamic parameters such as impact force and impact duration in the impact process [3]. Therefore, the analysis on the changes of acceleration signal when steel wheel imposes impact force on the elastic half-space is of great significance in analyzing the dynamic response of moving objects during impacting process and quantifying the impacting force and dynamic modulus of elastic half-space [4].

The impact process has a strong nonlinear characteristic, and it is influenced by many factors including initial conditions, material characteristics, and structure shape [5]. So a complete theoretical system of impact dynamics has not yet been formed [6]. To study the impact process, Newton first proposed the kinematic recovery coefficient to describe the change in the velocity before and after the collision of two objects. Poisson also proposed the dynamic collision recovery coefficient from the perspective of the momentum. Several scholars studied the collision recovery coefficient from the view of energy [7-9]. Several Chinese scholars conducted studies on the collision dynamics, and compared the applicable conditions of three collision coefficients with the accuracy of collision impact process [10-12]. Several scholars used kinematic recovery coefficient to evaluate the dynamic response of rockfall impacting the ground [13, 14]. Research has shown that the collision recovery coefficient can well describe the change of object motion before and after the collision, but it cannot describe the change of dynamic parameters such as force and acceleration during the collision.

* Corresponding author e-mail: liangnx@cqjtu.edu.cn.

The research on dynamic response in the impact process focuses on the field of contact mechanics. The basic theory for collision impact between elastomers was proposed by Hertz [15]. Based on Hertz's contact mechanics, domestic and foreign scholars conducted a lot of studies on impact dynamics between sphere and sphere or between sphere and plane or cylinder to cylinder, and obtained an accurate theoretical explanation [16-18, 5]. However, it is difficult in the study of line contact between cylinder and plane, and there is not yet an accurate and convenient solution available [6]. Several scholars proposed a nonlinear model of the relationship between impact and strain based on Hertz contact theory, which can be used to analyze the dynamic response of impact between cylinder and plane [15, 19, 20]. However, the implicit equation adopted in the theory makes it difficult to be applied in engineering. To make it accessible, many scholars proposed empirical formulas that adopt display equations, and the Palmgren formula is the most widely used one [21].

Although the Palmgren empirical formula has a high computational accuracy, it is mainly used for the dynamics process of impact between solid cylinder and plane. The steel wheel is a common cylindrical shell structure in engineering [22]. There is no evidence to prove that the impact between steel wheel and elastic half-space can be solved by using this formula. In this paper, a simulation model of steel wheel impacting the elastic half-space is established by adopting finite element method. Based on Palmgren formula, main influencing factors affecting dynamic process of steel wheel impacting the elastic half-space are determined and the acceleration of steel wheel is taken as the dependent variable, establishing the relationship between various influencing factors and the acceleration of steel wheel.

## 2. Methods and Materials

### *2.1. Method to determine main influencing factors of impact process*

To determine the influencing factors of dynamic response, simplify the model and determine the main influencing factors, the following assumptions to the model are made: (1) The elastic modulus of steel wheel differs greatly from that of elastic half-space, so the steel wheel is regarded as the rigid body; (2) In the impact process, the elastic half-space conforms to the condition of small strain; (3) In the impact process, there is only vertical force distributed on the contact surface while no horizontal force distributed; (4) The contact surface is smooth without frictional force. The impact dynamics model is established as shown in Figure 1.

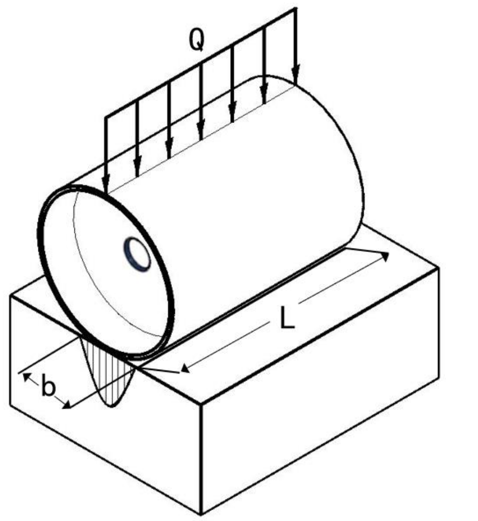


**Figure 1.** Schematic diagram of the steel wheel impacting the elastic half-space

According to the above assumptions, the maximum contact force is evenly distributed along the contact tessellation line, and its value can be solved by Hertz contact theory and Palmgreng empirical formula. When the cylinder imposes impact on the plane, the relationship between the impact force and the deformation of elastic half-space is shown in Formula (1).

$$F = K\varepsilon^{n} \tag{1}$$

where $F$ *is* the impact force, N; $\varepsilon$ is the deformation of elastic half-space, m; $n$ *is* the nonlinear index of cylinder contact, $n$ = 10/9 in the Palmgren elastic line contact model; $K$ *is* the equivalent stiffness of elastic contact, which is depended on the material and shape of contact body. According to Hertz contact theory and Palmgren elastic line contact model, the value of K is shown in Formula (2).

$$K = \frac{\pi}{\left(2\times 3.81\right)^{n}}\frac{E\times 10^{-6}}{1-\sigma^{2}}\left(1000L\right)^{\left(\frac{8}{9}\right)} \tag{2}$$

where $E$ *is* the elastic modulus of elastic half-space material, MPa; $\sigma$ is the Poisson's ratio of elastic half-space material; $L$ is the contact length of elastic line, mm.

The maximum impact ($F_m$) when cylinder impacts the elastic half-space is shown in Formula (3).

$$F_{m} = K\left[1000\left(n+1\right)\frac{m_{l}}{K}gh\right]^{\left(\frac{n}{n+1}\right)} \tag{3}$$

where $h$ is the impact height of steel wheel, mm; $m_l$ is the mass of cylinder, kg.

According to Newton's Second Law, the maximum impact acceleration ($a_m$) when cylinder impacts the elastic half-space is shown in Formula (4).

$$a_m = \frac{F_m}{m_l} = \frac{K}{m_l}\left[(n+1)\frac{m_l}{K}gh\right]^{\left(\frac{n}{n+1}\right)} \tag{4}$$

As can be seen from Formula (4), in the process that cylinder impacts the elastic half-space, the dynamic response is correlated with the length ($L$), mass ($m$), impact height ($h$) of cylinder as well as the elastic modulus ($E$) and Poisson's ratio ($\sigma$) of the material of elastic half-space.

This paper focuses on the relationship between the change of the material of elastic half-space and the change of dynamic response of steel wheel as well as relationship among the change of impact height, elastic modulus and the dynamic response of steel wheel. So the length ($L$) and mass ($m$) of the steel wheel are set to constant values.

*2.2. FEA model and materials*

According to the assumptions, a finite element model is established in the finite element analysis software ABAQUS, see Figure 2(a). In this model, the length of the steel wheel is 600 mm while the density is $7.8 \times 10^{-6}$ kg/mm$^3$. Calculation shows that the mass is 81.1 kg, the elastic modulus is 310 000 MPa, and the Poisson's ratio is 0.3.

The size of the elastic half-space is 6 000 × 3 000 × 3 000 mm and it adopts symmetry constraint to symmetric surfaces and fixed constraints to bottom surface and four sides. The density of elastic half-space is $2.4 \times 10^{-6}$ kg/mm$^3$, and the elastic modulus and Poisson's ratio are set as independent variables. The value range of elastic modulus is 500-8500 MPa, and Poisson's ratio is 0.2-0.4 [2, 23].

The 8-node hexahedron linear reduction integral element (C3D8R) and the modified quadratic tetrahedron element (C3D10M) can be chosen to simulate the impact process in ABAQUS software. According to the assumptions, the impact force in the finite element model is vertically downward and there is no large deformation. Therefore, in order to give consideration to calculation accuracy and simulation efficiency, the C3D8R element is selected as the grid element, and its total energy is basically 0 in the calculation process, thus there is no hourglass problem, so the calculation result is reliable. If the element C3D10M is selected, although certain accuracy can be improved, the calculation time will be increased by more than 6 times.

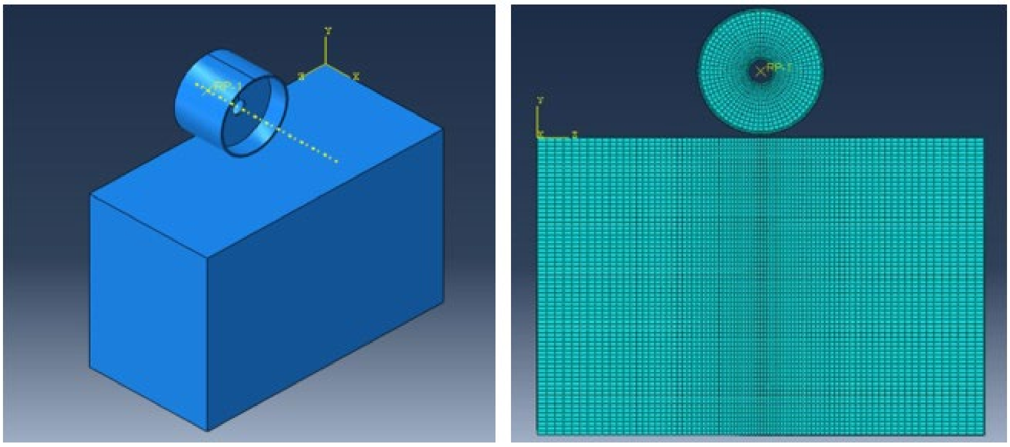

(a) The finite element model (b) The meshing method

**Figure 2.** The finite element model and meshing method

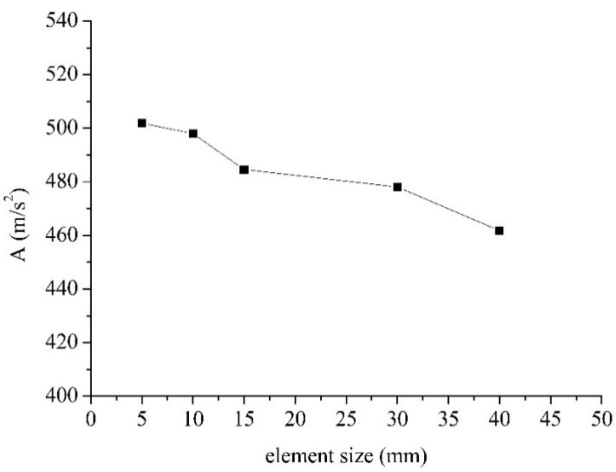


**Figure 3.** The sensitivity analysis results

 

In order to determine the mesh size, sensitivity analysis is carried out on the model. The elastic modulus of the elastic half-space is set as 6500 MPa and the Poisson's ratio is 0.3. The grid size is set to 40 mm, 30 mm, 15 mm, 10 mm and 5 mm respectively for simulation, and the results are shown in Figure 3. As can be seen from Figure 3, when the grid size is less than 10 mm, the change trend of acceleration response value slows down. Therefore, when the grid size is 5 mm, the calculation results tend to converge, but it takes a long time to calculate.

Then, set the grid along the Z direction, from 30 mm in the outermost part of the elastic half-space to 5 mm in the middle, and the other directions are set to 15 mm. The simulation result is basically the same as that when the grid is set to 5 mm, but the calculation time is reduced by about 28%. Therefore, the model is divided into grids as shown in Figure 2(b) in order to give consideration to both calculation accuracy and calculation speed.

## 3. Results and Discussion

### *3.1. Validation of the FEA model*

To verify the rationality of finite element model, the elastic modulus of elastic half-space is set to 6 500 MPa and the Poisson's ratio is set to 0.3. The impacting process is simulated as the impact height (*h*) is at 10 mm, 20 mm and 30 mm. Figure 4 shows the stress nephogram when steel wheel falls at height of 30 mm. As can be seen in Figure 4, when the steel wheel impacts the plane, the contact force is evenly distributed along the contact tessellation line, and only slightly increased at the steel wheel rim. Moreover, the contact stress shows elliptic distribution within the contact width (b), which is in line with Hertz contact theory.

The steel wheel is rigid body, so the dynamic response of all points on the steel wheel are the same when steel wheel impacts the elastic half-space. Take the top center of steel wheel as the test point, set the drop height to 10 mm, 20 mm and 30 mm, the elastic modulus to 2 500 MPa and 6 500 MPa, Poisson's ratio to 0.3, the velocity, stress and acceleration response of steel wheel are shown in Figures 5-7.

Figure 5 shows the velocity response during the impact process. As can be seen from Figure 5, when steel wheel falls at different height and impacts elastic half-space with different elastic modulus and Poisson's ratio, the velocity is only affected by falling height and hardly affected by elastic modulus and Poisson's ratio. According to the definition of kinematic recovery coefficient *e*, as shown in Formula 5, and the results have been showed in Table 1.

$$e = \frac{v_t}{v_0} \tag{5}$$

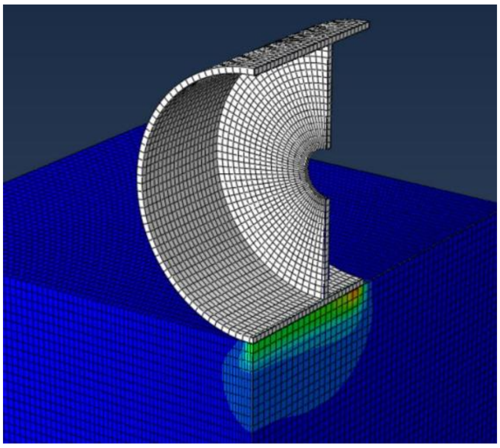

**Figure 4.** Stress nephogram in the impact process

Figure 6 shows the impact response curve when steel wheel impacts the half-space. As can be seen from Figure 6, during the impact process, the elastic modulus has a huge influence on impact force, which shows that greater the elastic modulus, greater the impact force. The elastic modulus also had an effect on impact duration, that is, the greater the elastic modulus, the shorter the impact duration; The Poisson's ratio of elastic half-space has little effect on impact force and impact time.

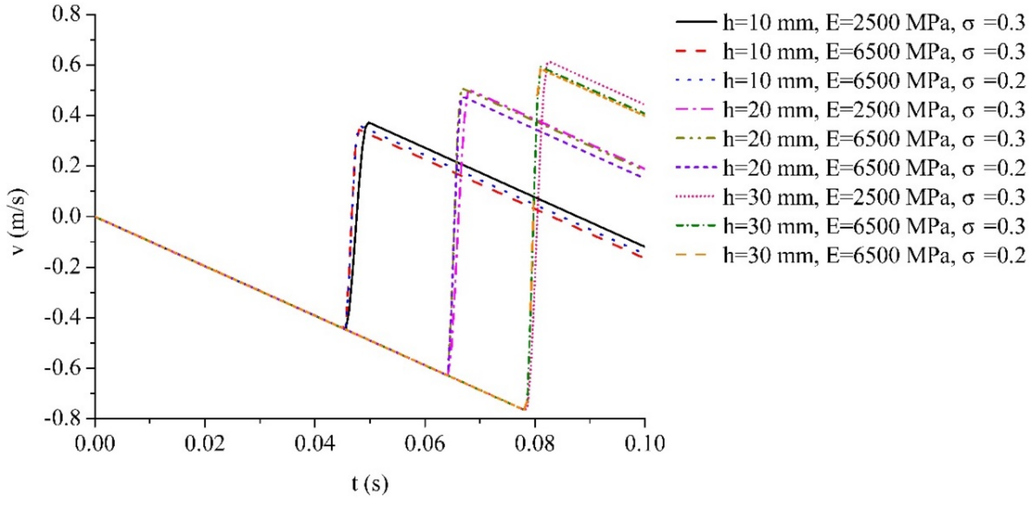


**Figure 5.** Curve of velocity response of steel wheel in the impact process

Figure 7 shows the curve of peak acceleration response of steel wheel in the impact process. As can be seen from Figure 7, the elastic modulus of elastic half-space has a great effect on acceleration response, that is, the greater the elastic modulus, the greater the peak acceleration; The Poisson's ratio of elastic half-space has little effect on peak acceleration response.

Compared between simulated velocity, impact and peak acceleration and the calculation result of acceleration and peak impact force according to Formula 3 and Formula 4 is as shown in Table 1.

As can be seen from Table 1, in the process that the elastic half-space with different elastic modulus and Poisson's ratio is impacted by the same steel wheel falling at different heights, the kinematic recovery coefficient before and after the impact is around 0.66. Therefore, the impact height of steel wheel and the material of elastic half-space does not affect the kinematic recovery coefficient of the impact system. The error between the simulation results of peak impact force and the calculation results of peak impact force by Formula (3) is less than 10%, and the error between the simulation results of peak acceleration and the calculation results of peak acceleration by Formula (4) is less than 20%, meeting the requirement of engineering use. Therefore, the finite element model is reasonable, and its simulation results can be used in the analysis of dynamic process of the steel wheel impacting the elastic half-space.

### *3.2. Effect law of the change of Poisson's ratio on acceleration response*

To find out how the change of Poisson's ratio affects the dynamic response of steel wheel, the impact process is simulated when elastic modulus is set to 500 MPa, 2 500 MPa, 4 500 MPa, 6 500 MPa, 8 500 MPa, Poisson's ratio is set to 0.2, 0.25, 0.3, 0.35, 0.4 and the falling height is set to 10 mm, 30 mm respectively. The Figure 8 shows the simulation result of peak acceleration change when the impact height is at 10 mm and 30 mm and the Poisson's rate changes from 0.2 to 0.4 with different elastic modulus.

As can be seen from Figure 8, when the elastic half-space with the same elastic modulus and Poisson's ratio of 0.2-0.4 is impacted by the same steel wheel falling at the same height, the peak acceleration of steel wheel has little change. Thus, the change of Poisson's ratio of elastic half-space has little effect on the peak acceleration of steel wheel.

Figure 9 shows the simulated result of impact duration when the impact height is at 10 mm and 30 mm and the Poisson's rate changes from 0.2 to 0.4 with different elastic modulus.

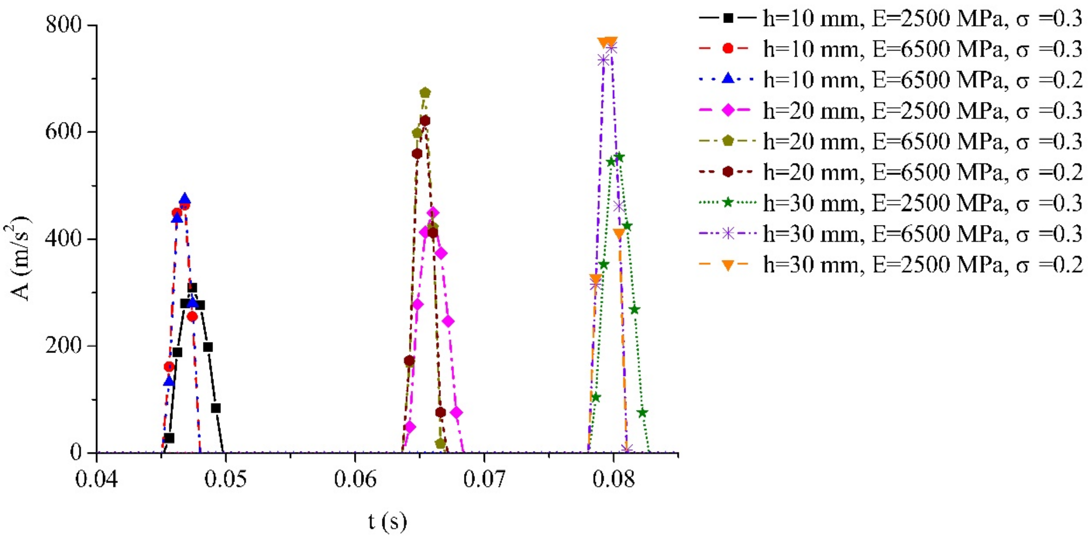


**Figure 7.** Curve of peak acceleration response of steel wheel in the impact process

**Table 1.** Comparison between the simulation results and the calculation results

| Impact height *h* /mm | Elastic modulus E/MPa | Steel wheel velocity v/(m·s$^{-1}$) Before the impact $v_0$ | After the impact $v_t$ | Recovery coefficient *e* | Impact force F/KN Theoretical value | Simulation value | Error | Acceleration A/(m·s$^{-2}$) Theoretical value | Simulation value | Error |
|---|---|---|---|---|---|---|---|---|---|---|
| 10 | 2500 | 0.44 | 0.30 | 0.68 | 31.07 | 33.28 | 7.11% | 383.22 | 308.72 | 19.44% |
| | 6500 | | 0.29 | 0.66 | 48.85 | 52.73 | 7.94% | 602.59 | 501.702 | 16.74% |
| 20 | 2500 | 0.63 | 0.43 | 0.68 | 44.75 | 49.15 | 9.83% | 551.96 | 449.01 | 18.65% |
| | 6500 | | 0.41 | 0.65 | 70.36 | 64.05 | 8.97% | 867.91 | 766.78 | 11.65% |
| 30 | 2500 | 0.77 | 0.50 | 0.65 | 55.39 | 55.26 | 0.23% | 683.26 | 592.610 | 13.27% |
| | 6500 | | 0.49 | 0.64 | 87.10 | 91.27 | 4.79% | 1074.36 | 895.20 | 16.68% |

 

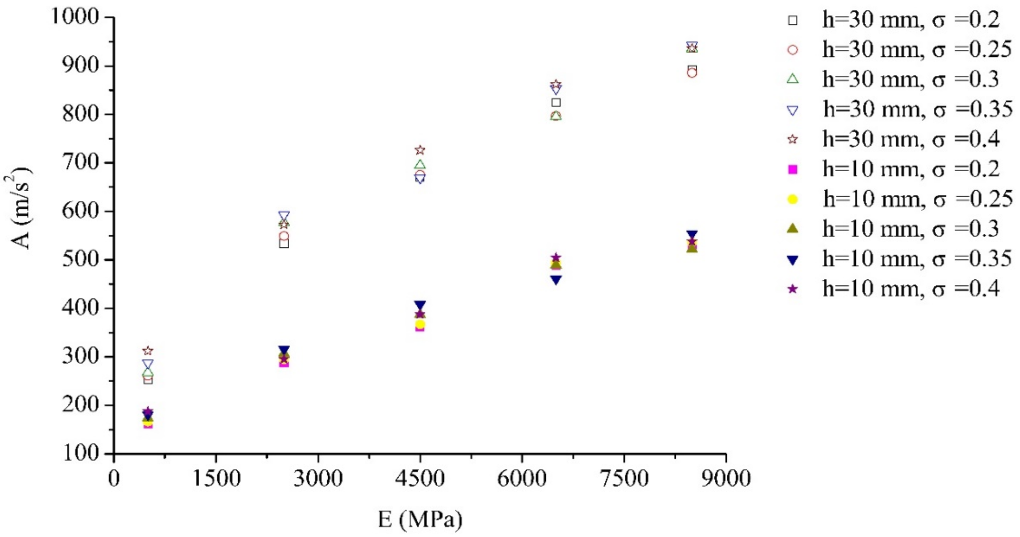


**Figure 8.** The relationship between peak acceleration and elastic modulus at different Poisson's ratio

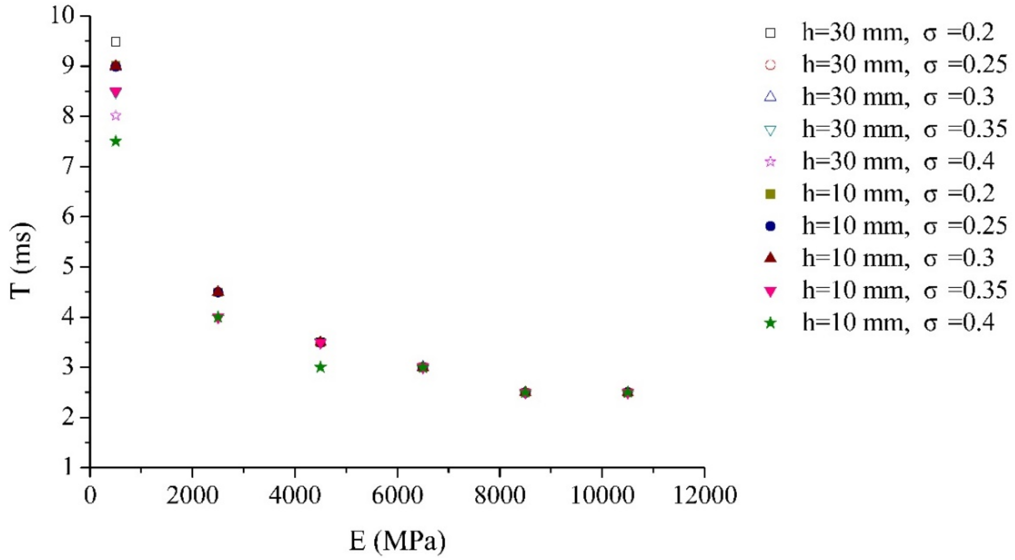


**Figure 9.** The relationship between impact duration and elastic modulus at different Poisson's ratios

As can be seen from Figure 9, when the elastic modulus is smaller than 2 500 MPa, Poisson's ratio change has a great effect on impact duration. However, when the elastic modulus is greater than 2 500 MPa, Poisson's ratio change has no effect on impact duration. Thus, the Poisson's ratio change of elastic half-space has little effect on the impact duration of steel wheel.

### *3.3. Effect law of elastic modulus change on acceleration response*

To find out how the change of elastic modulus of the material of elastic half-space affects the dynamic response of steel wheel, the elastic half-space with Poisson's rate is 0.3 and the elastic modulus is between 500 to 14 500 MPa impacted by the steel wheel at height of 10 mm to 40 mm is simulated. Figure 10 shows the relationship between peak acceleration and elastic modulus.

As can be seen from Figure 8, when the steel wheel impacts the elastic half-space at the same height, the peak acceleration increases with the increase of elastic modulus, and presents a quadratic nonlinear relationship. The fitting relationship between peak acceleration and elastic modulus at different heights is shown in Fit Curve10-Fit Curve40. From the curves it can be seen that the $R^2$ of the fitting curve is above 0.95, so the fitting curve has a high fitting accuracy.

### *3.4. Effect law of impact height change on acceleration response*

To find out how the change of impact height affects the dynamic response of steel wheel, the elastic half-space with the Poisson's rate is 0.3 and the elastic modulus is 500 MPa to 14 500 MPa is impacted by the steel wheel at height of 10 to 40 mm is simulated. Figure 9 shows the relationship between peak acceleration and impact height.

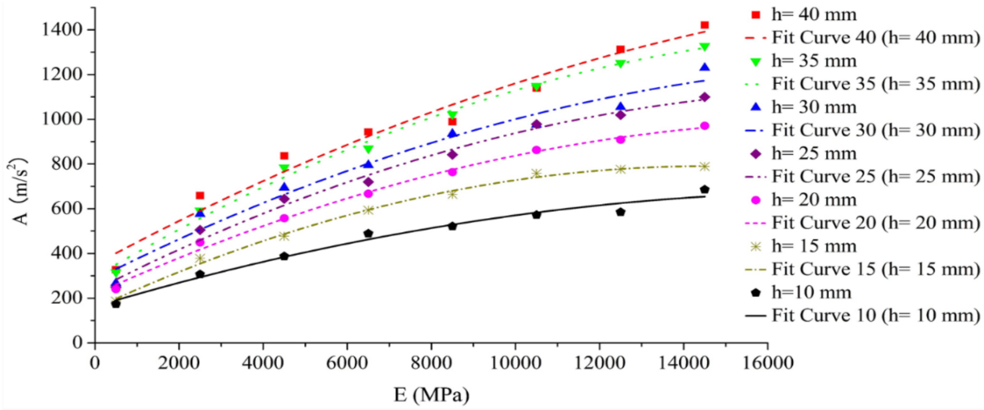


Fit Curve 10: $A = 163.22141 + 0.5596\ E - 1.52312 \times 10^{-6}\ E^2, R^2 = 0.97204$

Fit Curve 15: $A = 154.7949 + 0.08719\ E - 2.98888 \times 10^{-6}\ E^2, R^2 = 0.9941$

Fit Curve 20: $A = 218.4849 + 0.8539\ E - 2.34962 \times 10^{-6}\ E^2, R^2 = 0.99423$

Fit Curve 25: $A = 236.21379 + 0.09567\ E - 2.54728 \times 10^{-6}\ E^2, R^2 = 0.98453$

Fit Curve 30: $A = 283.50127 + 0.09476\ E - 2.30404 \times 10^{-6}\ E^2, R^2 = 0.95937$

Fit Curve 35: $A = 294.8684 + 0.11184\ E - 2.83986 \times 10^{-6}\ E^2, R^2 = 0.99013$

Fit Curve 40: $A = 350.88007 + 0.10147\ E - 2.04941 \times 10^{-6}\ E^2, R^2 = 0.96056$

**Figure 10.** The relationship between peak acceleration and elastic modulus

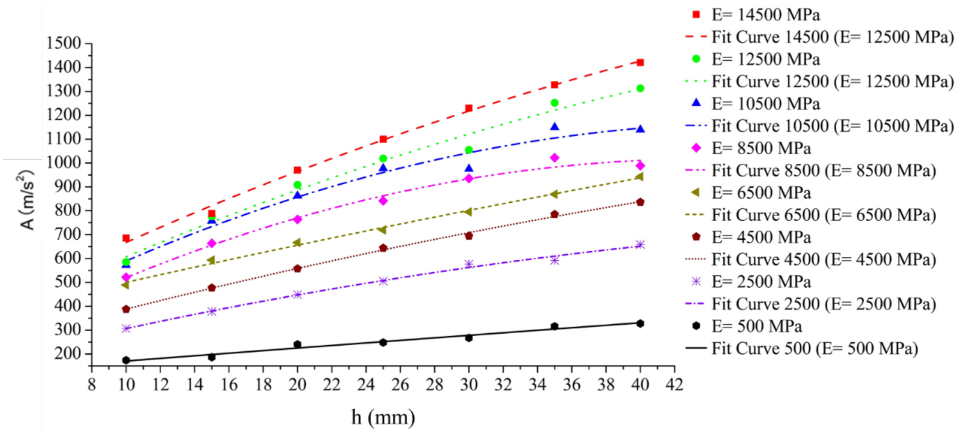


Fit Curve 500: $A = 115.85871 + 5.54435\ h - 0.00421\ h^2, R^2 = 0.95335$

Fit Curve 2500: $A = 140.17557 + 17.94033\ h - 0.12879\ h^2, R^2 = 0.99038$

Fit Curve 4500: $A = 197.43964 + 20.09649\ h - 0.102\ h^2, R^2 = 0.99671$

Fit Curve 6500: $A = 334.9895 + 17.01792\ h - 0.04847\ h^2, R^2 = 0.99364$

Fit Curve 8500: $A = 182.92507 + 38.0396\ h - 0.43356\ h^2, R^2 = 0.9806$

Fit Curve 10500: $A = 239.49214 + 39.13628\ h - 0.41175\ h^2, R^2 = 0.95443$

Fit Curve 12500: $A = 281.81214 + 34.8003\ h - 0.22721\ h^2, R^2 = 0.97367$

Fit Curve 14500: $A = 325.44071 + 36.41516\ h - 0.22199\ h^2, R^2 = 0.99457$

**Figure 11.** The relationship between peak acceleration and impact height

As can be seen from Figure 11, when the elastic modulus remains same, the peak acceleration increases with the increase of impact height, and presents a quadratic nonlinear relationship. The fitting relationship between peak acceleration and impact height at different heights is shown in Fit Curve500-Fit Curve14500 in Figure 11. From the curves, it can be seen that the $R^2$ of the fitting curve is above 0.95, so the fitting curve has a high fitting accuracy.

### *3.5. The effect law of the change of different influencing factors on acceleration response*

To analyze the effect of different influencing factors on the acceleration response of steel wheel, the elastic modulus of elastic half-space and the impact height of steel wheel are taken as the independent variables, while the peak acceleration of steel wheel as the dependent variable, the MAP diagram of the relationship between peak acceleration and different influencing factors is as shown in Figure 12.

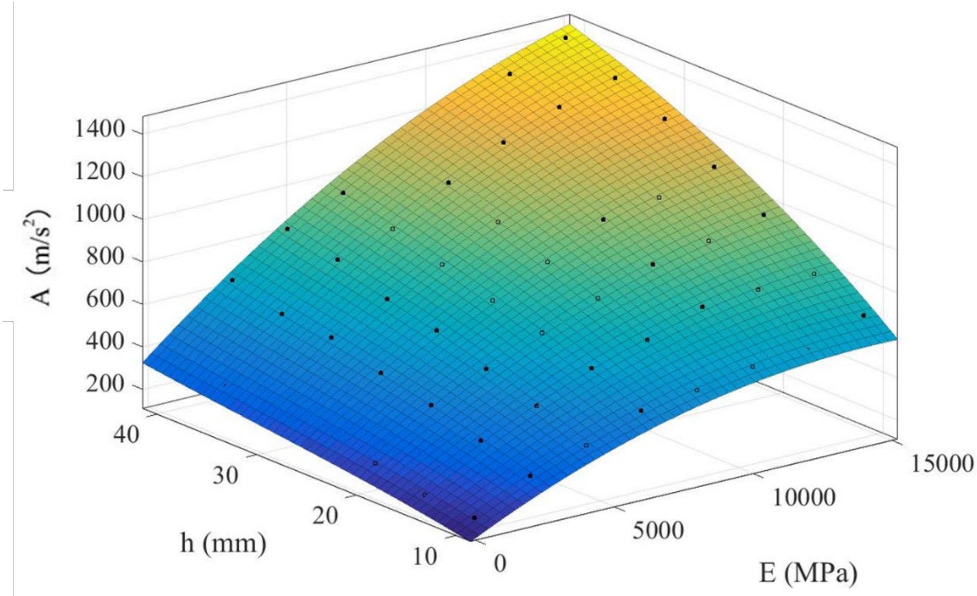


(a) MAP diagram

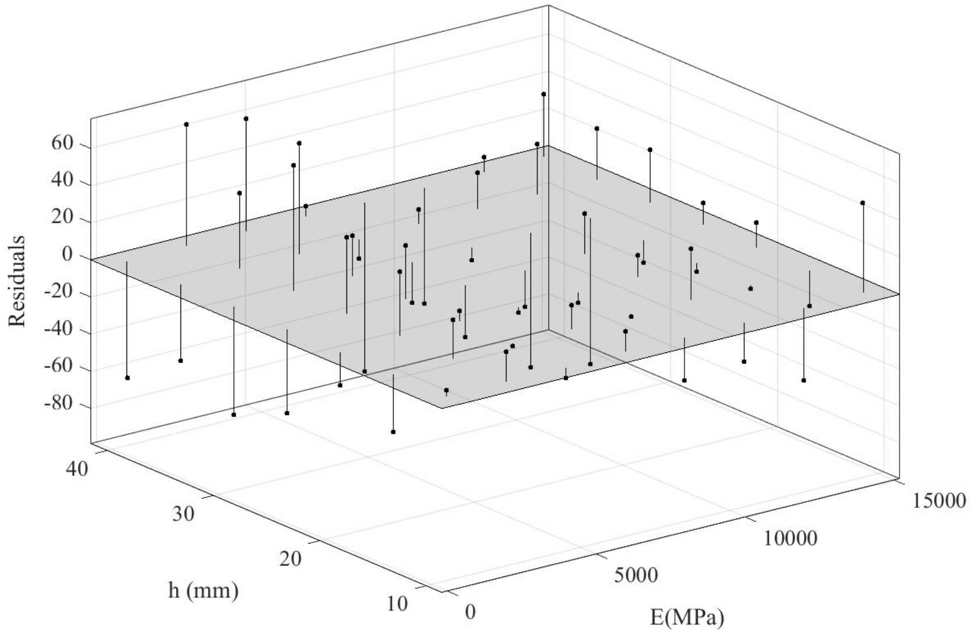


(b) Residual plot

**Figure 12.** The relationship between peak acceleration and different influence factors

Figure 12(a) shows the MAP diagram of the relationship between peak acceleration and different influence factors, and Figure 10(b) shows the residual plot of the fitting curves. As can be seen from Figure 12(b), the points depicted based on the elastic modulus and impact height of elastic half-space as the horizontal axis and the residual value as the vertical axis has no outliers. The points are randomly scattered up and down around a plane with a residual equal to 0, which shows that the fitting of the simulation values is well fitted with the regression surface. The fitting relationship is shown in Formula 6.

$$A = -30.36 + 0.05878E + 16.66h - 2.372\times10^{-6}E^2 + 0.001262Eh - 0.1972h^2 \quad (6)$$

To verify the correctness of the fitting results, 4 different impact height and 4 different elastic modulus are randomly selected to be calculated and simulated. The comparison result is as shown in the Table 2.

**Table 2.** Comparison between the simulation results and the calculation results

| Impact height h (mm) | Elastic modulus E (MPa) | Theoretical value (m/s$^2$) | Interpolation (m/s$^2$) | Simulation value (m/s$^2$) | Error (%) | |
|---|---|---|---|---|---|---|
| | | | | | Interpolation | Simulation value |
| 16 | 3500 | 597.1 | 433.1 | 464.9 | 27.1 | 22.1 |
| 24 | 7500 | 1060.4 | 790.5 | 903.9 | 25.5 | 14.8 |
| 32 | 10500 | 1446.9 | 1080.5 | 1132.4 | 25.3 | 21.7 |
| 40 | 15500 | 1956.9 | 1444.2 | 1587.7 | 26.2 | 18.9 |

As can be seen from Table 2, in the impact process combined with four randomly selected impact height and elastic modulus, all the theoretical values obtained from Formulas (1)-(4) are higher than the interpolation and simulation values and the error is around 25%, meeting the engineering requirements. So it can be used in the calculation of dynamic process of a particular steel wheel, which 600 mm long and 81.1 kg, impacting the elastic half-space.

## 4. Conclusion

1. A finite element model of elastic half-space impacted by steel wheel is established. According to Hertz contact theory and Palmgren empirical formula, it is confirmed that the main influencing factors of the dynamic response of impact process include the length and mass of steel wheel, the impact height, elastic modulus and Poisson's ratio of elastic half-space. The process of impacting the elastic half-space with elastic modulus of 2 500 MPa, 6 500 MPa and Poisson's ratio of 0.3 by the same steel wheel falling at heights of 10 mm, 20 mm and 30 mm is simulated respectively. The results show that the kinematic recovery coefficient of each impact process is consistent. The error between the simulation results of peak impact force and the calculation results of peak impact force by Formula (3) is less than 10%, and the error between the simulation results of peak acceleration and the calculation results of peak acceleration by Formula (4) is less than 20%, meeting the engineering requirements. So the finite element model is proved to be reasonable, and its simulation results can be used in the analysis of dynamic process of steel wheel impacting the elastic half-space;
2. The process of elastic half-space that the elastic modulus changes from 500 MPa to 8 500 MPa and the Poisson's rate changes from 0.2 to 0.4 impacted by steel wheel from the height of 10 mm and 30 mm is simulated. The simulation result shows that when the elastic modulus is smaller than 2 500 MPa, Poisson's ratio change has a great effect on impact duration and little effect on peak acceleration. However, when the elastic modulus is greater than 2 500 MPa, Poisson's ratio change has no effect on impact duration and no significant effect on peak acceleration;
3. The process of elastic half-space that the elastic modulus changes from 500 MPa to 14 500 MPa and the Poisson's rate is 0.3 impacted by steel wheel from the height from 10-40 mm is simulated. The results show that when the steel wheel impacted the elastic half-space at the same height, the peak acceleration increases with the increase of elastic modulus, and presents a quadratic nonlinear relationship;
4. Based on the simulation results, the elastic modulus of elastic half-space and the impact height of steel wheel is taken as the independent variables and the peak acceleration of steel wheel as the dependent variable, the MAP diagram and fitting formula of the relationship between peak acceleration and different influencing factors is made. Four different impact height and four different elastic modulus are randomly selected to be calculated and simulated, which shows that all the theoretical values are higher than the interpolation and simulation values and the error is around 25%, meeting the engineering requirements. So it can be used in the calculation of dynamic process of a particular steel wheel, which 600 mm long and 81.1 kg, impacting the elastic half-space.

## References

[1] Li, H. Impact and rebound of thin-walled structures on a rigid target. Hangzhou: Zhejiang University, 2018.
[2] Cao, Z.P., Liang, N.X., Cao, Y.W. Method for continuously testing pavement structural composite modulus. Journal of Harbin Institute of Technology, 2020, 52(3): 90-98.
[3] Chen, W.Z., Wang, B.W., Hu, X.Y. Acceleration signal processing by time domain integration. Journal of Huazhong University of Science and Technology (Natural Science Edition), 2010, 38(1): 1-4.
[4] Ismail, A., Zenasni, R., Amine, K.S.M., Ahmed, S. Effect of tempering temperature on the mechanical properties and microstructure of low alloy Steel DIN 41Cr4. Jordan Journal of Mechanical and Industrial Engineering, 2019, 13(1): 9-14.
[5] Wang, X.P., Lin, W.Z., Liu, G., Ma, S.J., Tong, R.T. Advance in impact force model research with evolution of newton restitution coefficient. Mechanical

Science and Technology for Aerospace Engineering, 2020, 39(10): 1526-1533.

[6] Machado, M., Moreira, P., Flores, P., Lankarani, H.M. Compliant contact force models in multibody dynamics: Evolution of the Hertz contact theory. Mechanism and Machine Theory, 2012, 53: 99-121.

[7] Stronge, W.J. Impact mechanics. Cambridge: Cambridge University Press, 2000.

[8] Wagg, D.J. A note on coefficient of restitution models including the effects of impact induced vibration. Journal of Sound and Vibration, 2007, 300: 1071-1078.

[9] Ivanov, A.P. Energetics of a collision with friction. Journal of Applied Mathematics and Mechanics, 1992, 564: 527-534.

[10] Yao, W.L., Yue, R. Advance in controversial restitution coefficient study for impact problems. Journal of Vibration and Shock, 2015, 34(19): 43-48.

[11] Dong, F.X., Hong, J.Z. Review of impact problem for dynamics of multibody system. Advances in Mechanics, 2009, 39(3): 352-359.

[12] Zhang, J.Z. The suitable situation of formula of coefficient of restitution for general rigid body of motion. Mechanics in Engineering, 2010, 32(3): 116-117.

[13] Ye, Y., Zeng, Y.W., Peng, Z.X., Sun, H.W., Ren, S.L., Wang, K. Experimental study on normal coefficient of restitution and fragmenting of marble spheres. Chinese Journal of Rock Mechanics and Engineering, 2018, 37(7): 1680-1690.

[14] Bi, R., Li, S.Y., Liu, G., Ren, J.X., Song, Y.J., Tsai, S.B. Investigating the effect of preimpact energy dissipation on coefficient of restitution regarding the slope-boulder interaction. Advances in Civil Engineering, 2021, 2021: 1-23.

[15] Johnson, K.L. Contact Mechanics. Cambridge: Cambridge University Press, 1985.

[16] Xu, G.H., Shen, W.C., Liu, Y.J. Measurement and calculation of impact stress in ball mills. Journal of Tsinghua University (Science and Technology), 1996, 36(4): 87-92.

[17] Li, L.Y., Thornton, C., Wu, C.Y. Impact behaviour of elastoplastic spheres with a rigid wall. Journal of Mechanical Engineering Science, 2000, 214(8), 1107-1114.

[18] Yin, M.G., Thibaut, C., Wang, L.W., Nelias, D., Zhu, M.H., Cai, Z.B. Impact-sliding wear response of 2.25Cr1Mo steel tubes: Experimental and semi-analytical method. Friction, 2021, 2021:1-19.

[19] Cândida, M.P., Amílcar, L.R., Jorge, A.A. A critical overview of internal and external cylinder contact force models. Nonlinear Dynamics, 2011, 63(4): 681-697.

[20] Lankarani, H.M., Nikravesh, P.E. Continuous contact force models for impact analysis in multibody systems. Nonlinear Dynamics, 1994,5(2): 193-207.

[21] Li, Y.G., Chen, T.N., Wang, X.P., Yu, K.P. Theoretical analysis and numerical simulation for impact noise due to collision of two cylinders. Journal of Vibration and Shock, 2014, 33(15): 162-173.

[22] Kachapi, S.H.H. Nonlinear vibration and frequency analysis of functionally graded- piezoelectric cylindrical nano-shell with surface elasticity. Jordan Journal of Mechanical and Industrial Engineering, 2018, 12(4): 293-312.

[23] Liu, B.Y. Specifications for design of highway asphalt pavement. Beijing: China Communications Press, 2017.